ORIGINAL PAPER

UNSTEADY MHD FLOW PAST AN IMPULSIVELY STARTED OSCILLATING VERTICAL PLATE WITH CONSTANT WALL TEMPERATURE AND VARIABLE MASS DIFFUSION IN THE PRESENCE OF HALL CURRENT

U. S. RAJPUT[1], NEETU KANAUJIA[2]

Manuscript received: 07.10.2016; Accepted paper: 14.02.2017;
Published online: 30.03.2017.

Abstract.*In the present paper, unsteady MHD flow past an impulsively started oscillating vertical plate with constant wall temperature and variable mass diffusion in the presence of Hall current is studied here. The fluid considered is an electrically conducting. The Laplace transform technique has been used to find the solutions for the velocity profile and skin friction. The velocity profile and skin friction have been studied for different parameters like Schmidt number, Hall parameter, magnetic parameter, mass Grashof number, thermal Grashof number, Prandtl number, and time. The effect of parameters is shown graphically and the value of the skin-friction for different parameters has been tabulated.*

Keywords: *MHD, Hall current, variable mass and constant wall temperature.*

1. INTRODUCTION

The study of MHD flow and Hall effect plays an important role in engineering and biological science. MHD flow models with Hall effect have been studied by a number of researchers, some of which are mentioned here. Datta and Jana [1] have studied oscillatory magnetohydrodynamic flow past a flat plate with Hall effects. Pop et al. [2] have studied Hall effect on magnetohydrodynamic boundary layer flow over a continuous moving flat plate.Katagiri [3] have studied the effect of Hall current on the magnetohydrodynamic boundary layer flow past a semi-infinite fast plate.Deka [4] has analyzed Hall effects on MHD flow past an accelerated plate. Some research articles related to MHD flow with oscillating plate are also mentioned here. Muthucumaraswamy [5] have analyzed mass transfer effect on isothermal vertical oscillating plate in the presence of chemical reaction. Deka et al. [6] have analyzed unsteady MHD flow past a vertical oscillating plate with thermal radiation and variable mass diffusion. Soundalgekar [7] has studied free convection effects on the oscillatory flow on an infinite vertical porous plate with constant suction. Further, Beg and Ghosh [8] have analyzed magneto-hydrodynamic radiation-convection with surface temperature. Soundalgekar [9] has studied oscillatory MHD channel flow and heat transfer. Deka [10] have analyzed thermal radiation and oscillating plate temperature effects on MHD unsteady flow past a semi-infinite porous vertical plate under suction and chemical reaction. Rajput and Kumar [11] have analyzed radiation effects on MHD flow through porous media past an impulsively started vertical oscillating plate with variable mass diffusion. Attia [12]

[1]University of Lucknow,Department of Mathematics and Astronomy, India.
E-mail: usrajput07@gmail.com; rajputneetulko@gmail.com.

has analyzed unsteady MHD flow and heat transfer of dusty fluid between parallel plates with variable physical properties. Rajput and Kumar [13] have studied MHD flow past an impulsively started vertical plate with variable temperature and mass diffusion. Rajput and sahu [14] have studied transient free convection MHD flow between two long vertical parallel plates with constant temperature and variable mass diffusion. Raptis et al. [15] have studied mass transfer effects subjected to variable suction or injection. We are considering MHD flow past an impulsively started oscillating vertical plate with constant wall temperature and variable mass diffusion in the presence of Hall current. The effect of Hall current on the velocity has been observed with the help of graphs, and the skin friction has been tabulated.

2. MATHEMATICAL FORMULATION

An unsteady viscous incompressible electrically conducting fluid past an impulsively started oscillating vertical plate is considered here. The plate is electrically non-conducting. The x axis is taken in the direction of the motion and *z* normal to it. A uniform magnetic field B is assumed to be applied on the flow. Initially, at time $t \leq 0$ the temperature of the fluid and the plate is T_∞ and the concentration of the fluid is C_∞. At time $t > 0$, the plate starts oscillating in its own plane with frequency ω. The temperature and the concentration of the plate are raised to T_w and C_w, respectively. Using the relation $\nabla \cdot B = 0$ for the magnetic field $\overline{B} = (B_x, B_y, B_z)$, we obtain B_y (say B_0) = constant, i.e. $B = (0, B_0, 0)$, where B_0 is externally applied transverse magnetic field. There will be two components of the momentum equation, which are mentioned hereafter. The usual assumptions have been taken into consideration. The geometric model of the flow problem is shown in Figure -1.

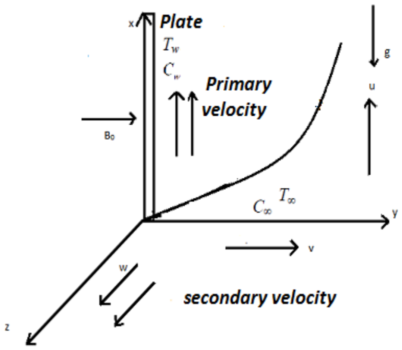

Figure 1. Physical Model

The fluid model is as under

$$\frac{\partial u}{\partial t} = \upsilon \frac{\partial^2 u}{\partial y^2} + g\beta(T - T_\infty) + g\beta^*(C - C_\infty) - \frac{\sigma B_0{}^2}{\rho(1+m^2)}(u + mw)\,, \tag{1}$$

$$\frac{\partial w}{\partial t} = \upsilon \frac{\partial^2 w}{\partial y^2} - \frac{\sigma B_0{}^2}{\rho(1+m^2)}(w - mu)\,, \tag{2}$$

$$\frac{\partial C}{\partial t} = D\frac{\partial^2 C}{\partial y^2}, \tag{3}$$

$$\frac{\partial T}{\partial t} = \frac{k}{\rho C_P}\frac{\partial^2 T}{\partial y^2}. \tag{4}$$

The following boundary conditions have been assumed:

$$\left.\begin{array}{l} t \le 0 : u = 0, w = 0, C = C_\infty, T = T_\infty, \text{for all the values of } y \\ t > 0 : u = u_0 \cos \omega t, w = 0, T = T_w, C = C_\infty + (C_w - C_\infty)\dfrac{u_0{}^2 t}{\upsilon} \text{ at } y = 0 \\ u \to 0, w \to 0, C \to C_\infty, T \to T_\infty \quad \text{as } y \to \infty \end{array}\right\} \tag{5}$$

Here u is the velocity of the fluid in x- direction (primary velocity), w - the velocity of the fluid in z- direction (secondary velocity), m - Hall parameter, g – acceleration due to gravity, β - volumetric coefficient of thermal expansion, β^* - volumetric coefficient of concentration expansion, t- time, C_∞ - the concentration in the fluid far away from the plate, C - species concentration in the fluid , C_w - species concentration at the plate, D - mass diffusion, T_∞ - the temperature of the fluid near the plate, T_w - temperature of the plate, T - the temperature of the fluid, k - the thermal conductivity, υ - the kinematic viscosity, ρ - the fluid density, σ - electrical conductivity, μ - the magnetic permeability, and C_P - specific heat at constant pressure. Here $m = \omega_e\tau_e$ with ω_e - cyclotron frequency of electrons and τ_e - electron collision time.
To write the Eqs. [1] – [4] in dimensionless from, we introduce the following non - dimensional quantities:

$$\left.\begin{array}{l} \bar{u} = \dfrac{u}{u_0}, \bar{w} = \dfrac{w}{u_0}, \bar{y} = \dfrac{yu_0}{\upsilon}, Sc = \dfrac{\upsilon}{D}, Pr = \dfrac{\mu C_P}{k}, M = \dfrac{\sigma B_0^2 \upsilon}{\rho u_0^2}, \bar{t} = \dfrac{tu_0{}^2}{\upsilon}, \\ Gr = \dfrac{g\beta\upsilon(T_w - T_\infty)}{u_0{}^3}, Gm = \dfrac{g\beta^*\upsilon(C_w - C_\infty)}{u_0{}^3}, \bar{C} = \dfrac{C - C_\infty}{C_w - C_\infty}, \theta = \dfrac{(T - T_\infty)}{(T_w - T_\infty)}. \end{array}\right\} \tag{6}$$

Here the symbols used are:
$\bar{u}$ - dimensionless velocity of the fluid in x- direction, $\bar{w}$ - dimensionless velocity of the fluid in z- direction, θ - the dimensionless temperature, $\bar{C}$ - the dimensionless concentration, Gr - thermal Grashof number, Gm - mass Grashof number, μ - the coefficient of viscosity, Pr - the Prandtl number, Sc - theSchmidt number, M - the magnetic parameter.

Equations (1), (2), (3) and (4) are transformed into the following dimensionless forms:

$$\frac{\partial \bar{u}}{\partial \bar{t}}=\frac{\partial^2 \bar{u}}{\partial \bar{y}^2}+Gr\theta+Gm\bar{C}-\frac{M(\bar{u}+m\bar{w})}{(1+m^2)}, \tag{7}$$

$$\frac{\partial \bar{w}}{\partial \bar{t}}=\frac{\partial^2 \bar{w}}{\partial \bar{y}^2}-\frac{M(\bar{w}-m\bar{u})}{(1+m^2)}, \tag{8}$$

$$\frac{\partial \bar{C}}{\partial \bar{t}}=\frac{1}{Sc}\frac{\partial^2 \bar{C}}{\partial \bar{y}^2}, \tag{9}$$

$$\frac{\partial \theta}{\partial \bar{t}}=\frac{1}{\Pr}\frac{\partial^2 \theta}{\partial \bar{y}^2}. \tag{10}$$

The corresponding boundary conditions become:

$$\left.\begin{array}{l}\bar{t}\le 0, \bar{u}=0, \vec{w}=0, \bar{C}=0, \theta=0, \ for\, all\, value\, of\ \bar{y}\\ \bar{t}>0, \bar{u}=\cos\bar{\omega}\bar{t}, \bar{w}=0, \theta=1, \bar{C}=\bar{t}\ at\ \bar{y}=0\\ \bar{u}\to 0, \bar{C}\to 0, \theta\to 0, \bar{w}\to 0\ as\ \bar{y}\to\infty.\end{array}\right\} \tag{11}$$

Dropping the bars and combining Equations (7) and (8), we get

$$\frac{\partial q}{\partial t}=\frac{\partial^2 q}{\partial y^2}+Gr\theta+GmC-\left(\frac{M}{1+m^2}(1-mi)\right)q, \tag{12}$$

$$\frac{\partial C}{\partial t}=\frac{1}{Sc}\frac{\partial^2 C}{\partial y^2}, \tag{13}$$

$$\frac{\partial \theta}{\partial t}=\frac{1}{\Pr}\frac{\partial^2 \theta}{\partial y^2}, \tag{14}$$

where $\mathrm{q}=\mathrm{u}+\mathrm{iw}$, with corresponding boundary conditions

$$\left.\begin{array}{l}t\le 0: q=0, \theta=0, C=0, \ for\, all\, value\, of\ y,\\ t>0: q=\cos\omega t, w=0, \theta=1, C=t, at\ y=0,\\ q\to 0, C\to 0, \theta\to 0, w\to 0\ as\ y\to\infty.\end{array}\right\} \tag{15}$$

Equations (12), (13) and (14), subject to boundary conditions (15), are solved by Laplace transform technique.

The solution obtained is as under

$$q=[\frac{1}{4}e^{-it\omega}(P_1+P_2-e^{-y\sqrt{a-i\omega}}P_3-e^{y\sqrt{a-i\omega}}P_4-e^{-y\sqrt{a+i\omega}+2it\omega}P_3-e^{y\sqrt{a+i\omega}+2it\omega}P_4)+\frac{1}{2a}Gr\{-e^{-\sqrt{a}y}(A_0)$$
$$+e^{\frac{at}{-1+\Pr}\sqrt{\frac{at}{-1+\Pr}}y}(1+A_{10}+A_{15}A_{11})\}+\frac{1}{4a^2}Gmy\{\frac{1}{y}A(1-Sc-e^{-\sqrt{a}y}t)+\sqrt{a}e^{-\sqrt{a}y}(A_3)-\frac{1}{y}2e^{\frac{at}{-1+Sc}\sqrt{\frac{at}{-1+Sc}}y}$$
$$B(1-Sc)\}-\frac{1}{2a}Gr\{-2A_{12}+e^{\frac{at}{-1+\Pr}\sqrt{\frac{at}{-1+\Pr}}y}(1+A_{13}+A_{15}A_{14})\}-\frac{1}{2a^2\sqrt{\pi}}Gm\sqrt{Sc}y\{\frac{-2\sqrt{\pi}B_{13}}{\sqrt{Sc}y}(1-Sc-$$
$$t)+a\{2e^{-\frac{Scy^2}{4t}}\sqrt{t}-\sqrt{\pi}\sqrt{Sc}y(1-B_{14})+\frac{1}{y}e^{\frac{at}{-1+Sc}\sqrt{\frac{at}{-1+Sc}}\sqrt{Sc}y}\sqrt{\pi}B_0(\sqrt{Sc}-\frac{1}{\sqrt{Sc}})\}\}]$$
$$C=\left[\left(t+\frac{Scy^2}{2}\right)Erf\left(\frac{\sqrt{Sc}y}{2\sqrt{t}}\right)-e^{-\frac{y^2}{4t}Sc}\frac{\sqrt{Sct}y}{\sqrt{\pi}}\right]$$
$$\theta=Erfc\left[\frac{\sqrt{\Pr}y}{2\sqrt{t}}\right].$$

The dimensionless skin friction at the plate $y = 0$ is computed by

$$\left(\frac{dq}{dy}\right)_{y=0} = \tau_x + i\tau_z$$

3. RESULTS AND DISCUSSION

The numerical values of velocity and skin friction are computed for different parameters like Hall parameter, mass Grashof number, Schmidt number, time, thermal Grashof number, magnetic field parameter, Prandtl number, and phase angle.The values of the main parameters considered are: m =1, 1.5, *2*; Gm= 50, 70, 100; Sc = 2.01, 3, 5*;* Pr = 0.71, 7; $\omega t = 30^\circ, 45^\circ, 60^\circ$; Gr = 10, 20, 30; M = 2, 3, 4; t = 0.15, 0.2, 0.25.

Figures 2, 3, 7, and 8 show that primary velocity increases when m, Gm, Gr, and t are increased. In this case u increases with m. It means Hall current has increasing effect on the flow of the fluid along the plate. Figures 4, 5, 6, and 9 show that primary velocity decreases when M, Sc, Pr, and ωt are increased. And figures 11, 12 15, and 16 show that the secondary velocity increases when Gm, M, Gr and t are increased. Figures 10, 13, 14 and 17 show that secondary velocity decreases when m, Sc, Pr, and ωt are increased. Here w decreases when m is increased; this implies that the Hall parameter slows down the transverse velocity.

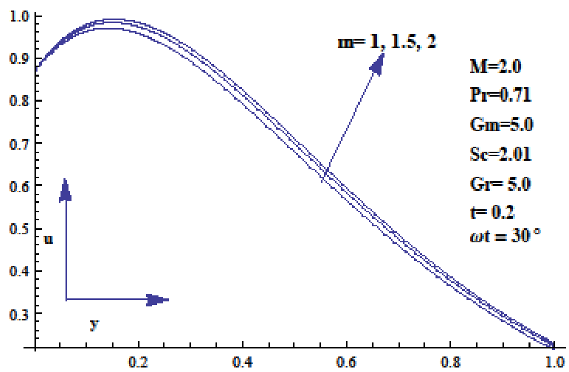

Figure 2. Velocity profile *u* for differentvalues of *m*.

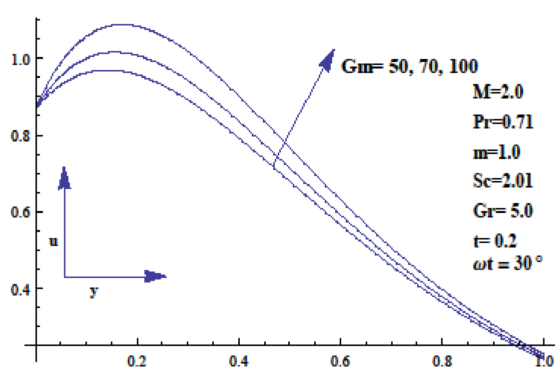

Figure 3. Velocity profile *u* for different values of *Gm*.

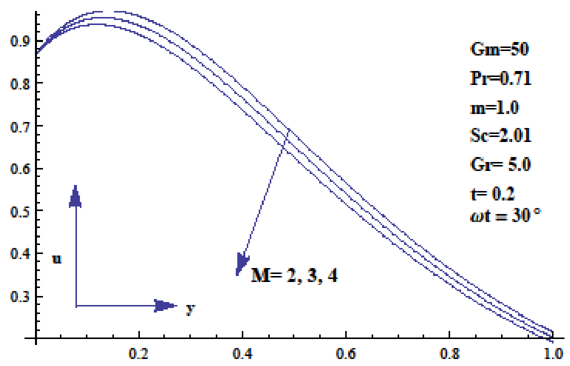

Figure4. Velocity profile *u* for differentvalues of *M*.

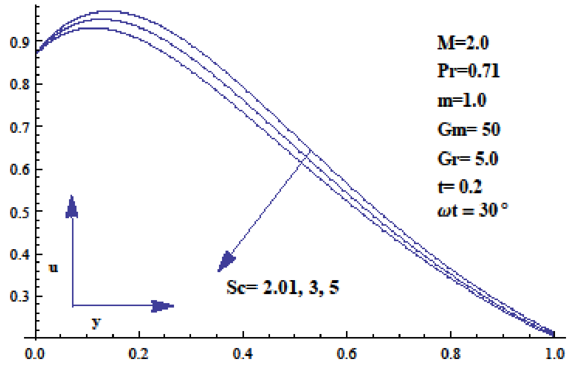

Figure 5. Velocity profile *u* for differentvalues of *Sc*.

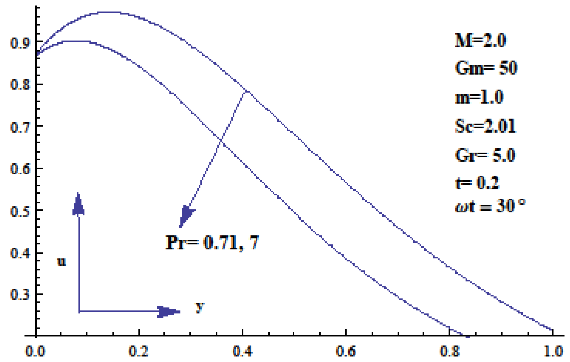

Figure 6. Velocity profiles *u* for differentvalues of *Pr*.

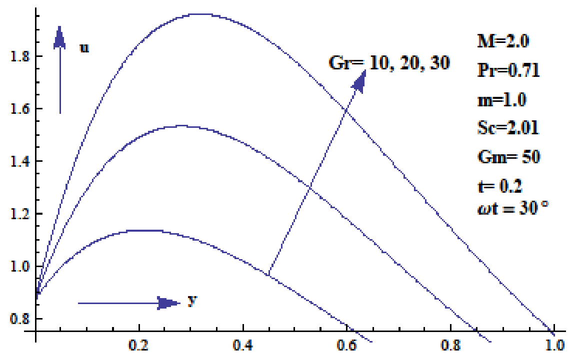

Figure 7. Velocity profile *u* for different values of *Gr*.

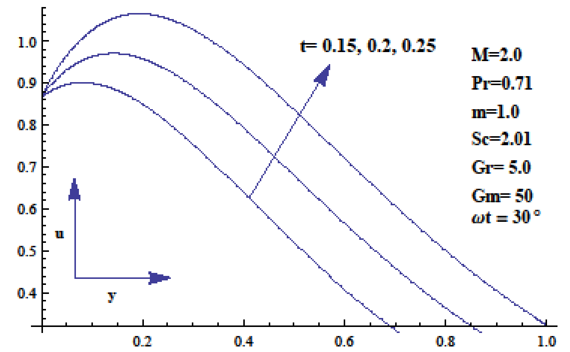

Figure 8. Velocity profile *u* for different values of *t*.

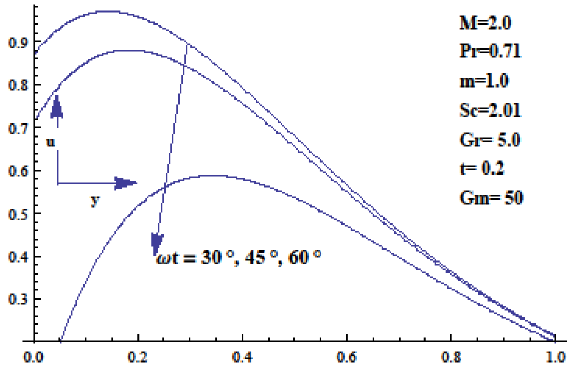

Figure 9. Velocity profile *u* for different values of ωt.

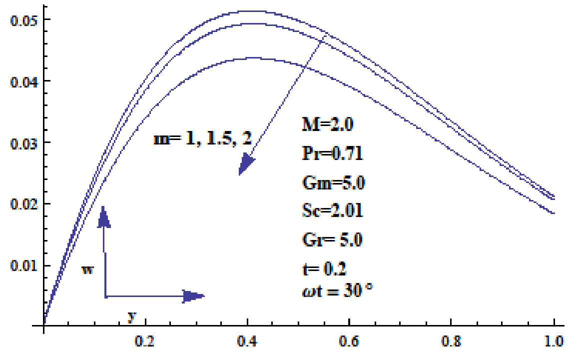

Figure10. Velocity profile *w* for differentvalues of *m*.

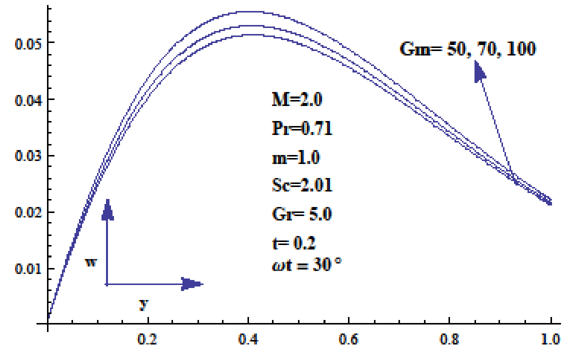

Figure11. Velocity profile *w* for differentvalues of *Gm*.

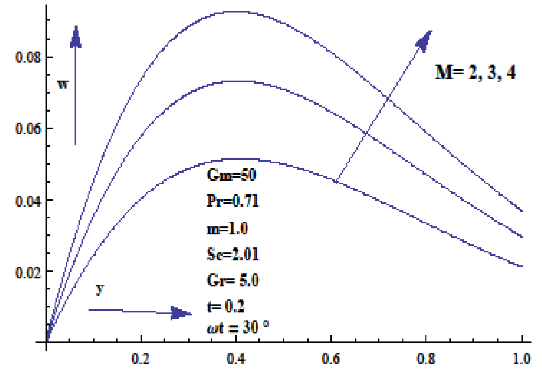

Figure12. Velocity profile *w* for different values of *M*.

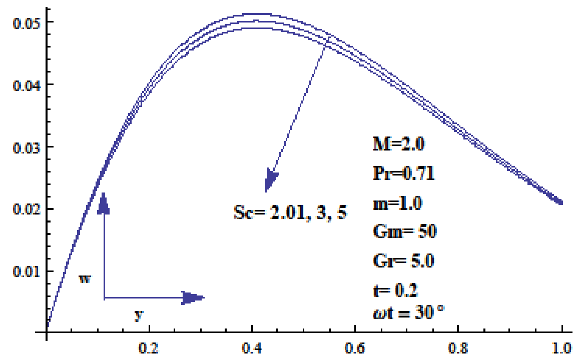

Figure13. Velocity profile *w* for differentvalues of *Sc*.

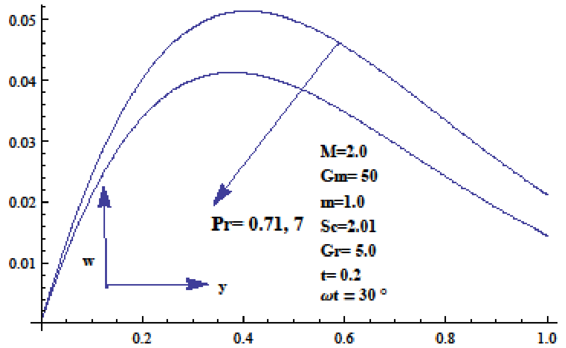

Figure 14. Velocity profile *w* for different values of *Pr*.

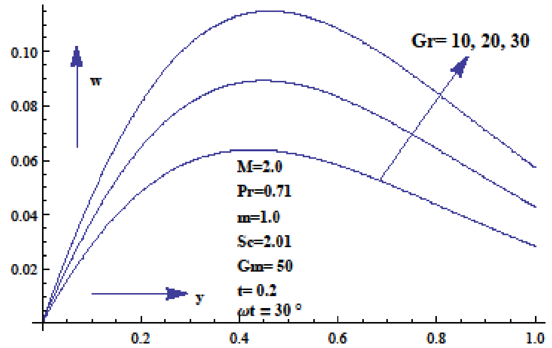

Figure15. Velocity profile *w* for different values of *Gr*.

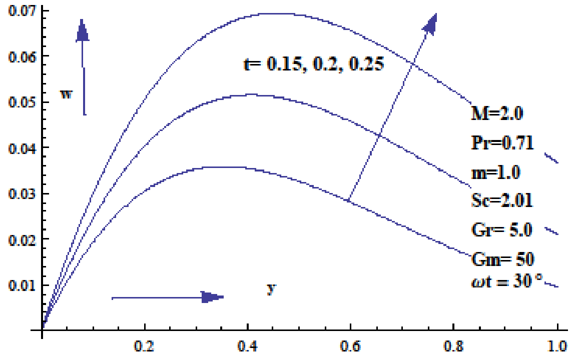

Figure16. Velocity profile *w* for different values of *t*.

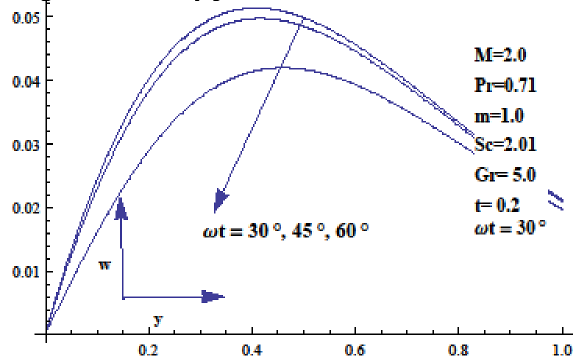

Figure17. Velocity profile *w* for different values of ωt.

Table 1.Skin friction.

m	*Gr*	*Gm*	*M*	*Sc*	*Pr*	*ωt(in degree)*	*t*	τ_x	τ_z
1.0	5.0	50	2.0	2.01	0.71	30	0.2	1.6399	0.2859
1.0	5.0	50	2.0	2.01	7.00	30	0.2	0.9994	0.2522
1.0	10	50	2.0	2.01	0.71	30	0.2	2.9598	0.3315
1.0	20	50	2.0	2.01	0.71	30	0.2	5.5995	0.4226
1.0	30	50	2.0	2.01	0.71	30	0.2	8.2393	0.5137
1.5	5.0	50	2.0	2.01	0.71	30	0.2	1.7525	0.2709
2.0	5.0	50	2.0	2.01	0.71	30	0.2	1.8183	0.2384
1.0	5.0	70	2.0	2.01	0.71	30	0.2	2.1873	0.2946
1.0	5.0	100	2.0	2.01	0.71	30	0.2	3.0083	0.3077
1.0	5.0	50	3.0	2.01	0.71	30	0.2	1.4883	0.4142
1.0	5.0	50	4.0	2.01	0.71	30	0.2	1.3383	0.5336
1.0	5.0	50	2.0	3.0	0.71	30	0.2	1.4848	0.2812
1.0	5.0	50	2.0	5.0	0.71	30	0.2	1.2982	0.2763
1.0	5.0	50	2.0	2.01	0.71	30	0.15	0.9029	0.2335
1.0	5.0	50	2.0	2.01	0.71	30	0.2	1.6399	0.2859
1.0	5.0	50	2.0	2.01	0.71	30	0.25	2.3768	0.3402
1.0	5.0	50	2.0	2.01	0.71	45	0.2	2.1810	0.2647
1.0	5.0	50	2.0	2.01	0.71	90	0.2	4.4075	0.1660

4. CONCLUSIONS

The conclusions of the study are as under:

1. Primary velocity increases with the increase in thermal Grashof number, Hall parameter, mass Grashof number and time.
2. Primary velocity decreases with the increase in Prandtl number, magnetic field parameter, Schmidt number, and phase angle.
3. Secondary velocity increases with increase in thermal Grashof number, mass Grashof number, time, and magnetic field parameter.
4. Secondary velocity decreases with the increase in Hall parameter, Prandtl number, Schmidt number and phase angle.
5. Skin fraction τ_x decreases with increase in Schmidt number, Prandtl number, and magnetic field parameter. It increases with thermal Grashof number, mass Grashof number, Hall parameter, time, and phase angle. Further, τ_z increases with increase in thermal Grashof number, mass Grashof number, time, and magnetic field parameter. And it decreases with Prandtl number, Hall parameter, Schmidt number, and phase angle.

REFERENCES

[1] Datta,N., Jana, R.N., *J. Phys. Soc. Japan*, **40**, 14, 1976.
[2] Pop,I., Watanabe,T., *Acta Mech.*,**108**,35, 1995.
[3] Katagiri,M., *Journal of the Physical Society of Japan*,**27**(4),1051, 1969.
[4] Deka,R.K.,*Theoret. Appl. Mech.*,**35**(4),333, 2008.
[5] Muthucumaraswamy,R., Janakiraman,B.,*Int. J. Appl. Math. &Mechanics*,**4**(1),66, 2008.
[6] Deka,R.K., Neog,B.C.,*Chamchuri Journal of Mathematics*,**1**(2),79, 2009.
[7] Soundalgekar, V.M.,*Astrophysics and Space Science*,**64**, 165, 1979.
[8] Beg,A.O., Ghosh,S.K., *Int. J. Appl. Math. &Mechanics*,**6**(6),1, 2010.
[9] Soundalgekar,V.M., *Indian Journal of Pure and Applied Mathematics*, **15**,819, 1984.
[10] Sharma, S.,Deka, R.K.,*Int. J. Phys. &Math. Sci.*,**2**(2), 33, 2012.
[11] Rajput,U.S., Kumar, S., *ARPN J. Engin&Appl. Sci.*,**7**(1), 108,2012.
[12] Attia,H.A., *Applied Mathematical Modelling*,**26**, 863, 2002.
[13] Rajput,U.S., Kumar, S., *Applied Mathematical sciences*,**5**(3),149, 2011.
[14] Rajput,U.S., Sahu, P.K., *Int. Journal of Math. Analysis*,**5**(34), 165, 2011.
[15] Kafousias,N.G.,Raptis,A.A., *Rev. Roum. Sci. Techn. Mec.Apl.*,**26**, 11, 1981.

APPENDIX

$P_1 = e^{-y\sqrt{a-i\omega}} + e^{y\sqrt{a-i\omega}}$, $P_2 = e^{-y\sqrt{a+i\omega+2i\omega}} + e^{y\sqrt{a+i\omega+2i\omega}}$, $P_3 = Erf[\frac{y-2t\sqrt{a-i\omega}}{2t}]$, $P_4 = Erf[\frac{y+2t\sqrt{a-i\omega}}{2t}]$, $A_0 = (1+A_1+e^{2\sqrt{a}y}A_2)$, $A_1 = Erf[\frac{1}{2\sqrt{t}}2\sqrt{a}t-y]$,

$A_2 = Erf[\frac{1}{2\sqrt{t}}2\sqrt{a}t+y]$, $A_3 = \left(1+e^{2\sqrt{a}y}+A_1-e^{2\sqrt{a}y}A_2\right)$, $A_{10} = Erf[\frac{2\sqrt{\frac{a\Pr}{-1+\Pr}}t-y}{2\sqrt{t}}]$, $A_{11} = Erf[\frac{2\sqrt{\frac{a\Pr}{-1+\Pr}}t+y}{2\sqrt{t}}]$, $A_{12} = Erfc[\frac{\sqrt{\Pr}y}{2\sqrt{t}}]$, $A_{13} = Erf[\frac{2\sqrt{\frac{a}{-1+\Pr}}t-\sqrt{\Pr}y}{2\sqrt{t}}]$,

$A_{14} = Erf[\frac{2\sqrt{\frac{a}{-1+\Pr}}t+\sqrt{\Pr}y}{2\sqrt{t}}]$, $A_{15} = e^{2\sqrt{\frac{a\Pr}{-1+\Pr}}y}$, $B = 1+B_{17}+B_{11}-B_{17}B_{12}$, $B_0 = 1+B_{17}+B_{15}-B_{17}B_{16}$, $B_{11} = Erf[\frac{2\sqrt{\frac{aSc}{-1+Sc}}t-y}{2\sqrt{t}}]$, $B_{12} = Erf[\frac{2\sqrt{\frac{aSc}{-1+Sc}}t+y}{2\sqrt{t}}]$,

$B_{13} = [-1+Erf\frac{\sqrt{Sc}y}{2\sqrt{t}}]$, $B_{14} = Erf\frac{\sqrt{Sc}y}{2\sqrt{t}}$, $B_{15} = Erf[\frac{2\sqrt{\frac{a}{-1+Sc}}t-\sqrt{Sc}y}{2\sqrt{t}}]$, $B_{16} = Erf[\frac{2\sqrt{\frac{a}{-1+Sc}}t+\sqrt{Sc}y}{2\sqrt{t}}]$, $B_{17} = e^{2\sqrt{\frac{aSc}{-1+Sc}}y}$, $a = \frac{M}{1+m^2}(1-im)$,